# A Soft Reprogrammable Permanent Magnet for Magnetic Soft Robots

Günay Züngör[1], Can Berkay Akkaya[1], Tommaso Ranzani[2] *Member, IEEE,* and Evren Samur[1] *Senior Member, IEEE,*

***Abstract*—Magnetic soft robots promise unprecedented medical applications due to their untethered motion and control capabilities. These magnetic soft robots, which are navigated by external magnetic sources, can be designed to change their shape or mechanical properties under magnetic fields. However, keeping the modified state constant often requires a continuous power supply with high energy consumption. Changing the magnetic properties of soft magnetic robots can overcome this energy demand. To this end, we present a novel soft and reprogrammable permanent magnet whose magnetization can be remotely switched on and off by a short-duration, low-energy external magnetic pulse. It is suitable for on-board use in magnetic soft robots, either to modify the magnetic properties of such robots or to actuate certain functionalities. Based on this concept, two untethered millimeter-scale magnetic soft robots are developed for applications in capsule endoscopy and medical grasping. The predominant feature of the proposed robots is that, apart from navigation, only state change requires an external power supply, and state retention is enabled by the onboard reprogrammable permanent magnet. The proposed novel magnet allows soft magnetic robots to perform specific tasks without physical tethering by enabling remote state change. The presented concept opens new opportunities for magnetic soft robots to achieve energy-efficient, untethered operation with remotely programmable states, offering significant potential for advanced biomedical applications.**

***Index Terms*—Soft Robot Designs and Applications, Robotic Soft Materials, Magnetic Robots, Medical Robots and Systems**

## I. Introduction

Magnetic soft materials find broad application areas such as small-scale untethered soft robots [1]–[6], metamaterials and origami robots [7]–[9], and flexible electronics and sensors [6], [10]–[12]. Small-scale, mobile magnetic soft robots, operating independently or within a continuous system, hold significant potential for facilitating medical procedures, both for diagnosis and treatment [13], [14]. These miniature and flexible robotic devices can be remotely controlled through wireless power transfer, even within the human body [15]. This non-intrusive accessibility in tight and enclosed spaces, offered by these small-scale untethered robots, opens up possibilities for a range of applications, including micro-factories [16], bio-sensing [17], and various healthcare applications [18]–[20]. These applications encompass targeted drug delivery [19], [21] and minimally invasive surgery [18]–[20] as well.

Magnetic soft robots commonly hinge on electromagnets (EMs) or permanent magnets (PMs) for motion and control. EMs are great for controllability but require a continuous power supply. Conversely, PMs do not require a power source. However, bulky industrial robotic arm setups are required to control the direction of the magnetic field of PMs [22], [23]. Magnetic soft robots, which are navigated by either EMs or PMs, can be designed to change their shape or mechanical properties under magnetic fields. However, keeping the modified properties constant often requires a continuous power supply with high energy consumption. Changing the magnetic properties of soft magnetic robots can overcome this energy demand. Reprogramming of magnetic properties, in the current state of the art, is performed by heating above the Curie temperature of magnetic particles where the magnetic domains of the particles are reoriented by an applied external magnetic field. The heat requirement makes *in-vivo* magnetic reprogramming currently impossible.

An alternative method for actuating soft robots is the use of electro-permanent magnets (EPMs) [24]–[31]. EPMs reduce the energy consumption associated with EMs and improve the controllability of PMs. EPMs use permanent magnets as the source of the magnetic field, and a coil is used to control the state of this permanent magnet assembly by applying pulses. By changing the direction of one of the two magnets inside, the magnetic fields of the magnets support or dampen each other, resulting in an ON and OFF state. In the ON state, the magnetization direction of both magnets is the same, resulting in the source of a net magnetic vector. In the OFF state, the net magnetic force exerted by the EPM is zero because the magnetic fields of the two magnets cancel each other out. Because EPMs are rigid and rely on tethered power transmission, they are suitable for external power supplies. However, the fact that they are rigid and tethered poses a challenge for their on-board use in magnetic soft robots, which may be necessary to change the magnetic properties of such robots.

In this study, we propose a novel soft and reprogrammable permanent magnet (srPM) that is suitable for on-board use in magnetic soft robots either to modify the magnetic properties of such robots or to actuate certain functionalities. We present the design and development of the srPM and its use in two medical applications: (1) a soft magnetic capsule for targeted drug delivery and (2) a soft grasper for remote and untethered manipulation. The srPM has two controllable states, ON and

Manuscript received March 22, 2025; revised June 29, 2025; Accepted: September 16, 2025.This paper was recommended for publication by Editor Cecilia Laschi upon evaluation of the Associate Editor and Reviewers' comments. This project was supported by the Boğaziçi University Research Fund grant number 19782, and the Boğaziçi University Robotics and AI Laboratories Project (ROYAL) funded by the Presidency of Strategy and Budget of the Republic of Türkiye. We thank Assoc. Prof. Mustafa Öztürk from the Department of Physics at Gebze Technical University, and Uğur Topal from the Magnetism Laboratory at TÜBİTAK-UME for the VSM analysis. We thank Boğaziçi Center for Targeted Therapy Technologies, CT3 for the SEM.

[1]G. Züngör, C. B. Akkaya and E. Samur are with the Department of Mechanical Engineering, Boğaziçi University, İstanbul, Türkiye. [2]T. Ranzani is with the Department of Mechanical Engineering, Boston University, Boston, MA 02215, USA. gunay.zungor@bogazici.edu.tr

Digital Object Identifier (DOI): see top of this page.

OFF, in which it exerts significant and near-zero magnetic flux, respectively. The srPM can change state with a short duration, low energy external magnetic pulse. This novel concept of remote and untethered magnetic reprogramming and reconfiguration of small-scale soft robots goes beyond the current state of the art. The magnetic capsule based on the srPM is made entirely of soft components that promise active functions for targeted drug delivery, biopsy and therapeutics. The srPM-based grasper takes advantage of magnetic forces to open and close a gripper. It can be used for biopsy or fixation. The design, characterization and evaluation of the novel srPM, and the development of two new magnetic soft robots based on the srPM are presented in this paper.

### *A. Literature Review on Reprogrammable Magnetic Soft Robots*

Different strategies have been proposed to enable facile reprogramming of the magnetization patterns of magnetic materials. Based on the physical alignment and fixing of the magnetic particles during curing via lithographic or 3D printing techniques, magnetic programming approaches are introduced for encoding discrete 3D magnetization profiles in small-scale soft materials [1], [5], [6].

Alapan et al. [32] proposed a new approach that enables magnetic programming by heating above the Curie temperature of the ferromagnetic particles and reorienting magnetic domains with an external magnetic field applied during cooling. Their soft machines are composed of chromium dioxide (CrO2) microparticles with an average diameter of 10 $\mu$m embedded in a PDMS elastomer. CrO2 is a ferromagnetic material with a Curie temperature of around 118 °C. The proposed laser-based heat-assisted magnetization strategy enables local reprogramming with a spatial resolution of 38 $\mu$m.

G. Dong et al. [33] developed a magnetic vitrimer with magnetic particles mixed with a polymer network containing abundant dynamic covalent bonds. When the temperature is elevated to the exchange temperature of covalent bonds, the viscous magnetically responsive material undergoes large deformations. Magnetic vitrimer is produced of epoxy monomers stoichiometric mixtures of two sulfhydryls that are embedded with magnetic particles (Fe3O4) into the polymer matrix.

To reprogram magnetic materials, phase-change materials with relatively low melting temperatures, such as polyethylene glycol [34] or polycaprolactone [35], are also used to encapsulate the magnetic particles in the polymeric matrix.

W. Li et al. [36] proposed a self-vectoring electromagnetic soft robot demonstrating shape morphing and locomotion capabilities. It is designed with two magnetic coils, a planar spiral, and a 3D helix, which corresponds to a vertical flux actuator (module V) and a horizontal flux actuator (module H), respectively. The square shape of the two actuator modules allows them to assemble in different configurations.

Sun *et al.* present a dynamic reprogrammable magnetic soft machine (drMSM) including a flexible resonant circuit [37]. Reprogramming is achieved through addressable heating of specific regions in the machine. The machine consists of multiple branches of an inductor, a capacitor, and a resistance wire connected in series. By adjusting the capacitance in each branch, distinct resonant frequencies are defined. The heating field selectively targets and heats the branches that resonate at those frequencies. As the low-melting alloy melts, the NdFeB particles within the liquid chamber align with the applied magnetic field.

In 2025, Sodomka and Mach made electro-permanent elastomer (EPE) that can be switched ON and OFF similarly to an electro-permanent magnet [38]. Two ferromagnetic materials, namely, NdFeB and strontium ferrite (SF-D360) are mixed with Dragon Skin FX-PRO. The size of the sample is 17x17x2.5 mm. They achieved 67 mT of remanent magnetization in the ON and 2.1 mT remanent magnetization in the OFF state. Their EPE needs 620 mT to change between states, which is quite challenging to apply externally.

Johnson and Kramer-Bottiglio proposed a compliant EPM that mixes AlNiCo and NdFeB magnetic powders in a matrix [39]. Although they have achieved a soft EPM that can carry its own weight and vice versa in the OFF state, the magnetization in OFF states is not close to zero because mixing magnetic particles leads to magnetic interaction of the adjacent powders [40], [41]. Besides, the magnetic flux density is not close to zero on the surface at the OFF state due to the lack of the directed alignment of the magnetic field that is normally achieved by magnetic caps of EPMs. Therefore, there is still a gap in the field in terms of efficiently and remotely reprogrammable magnetic soft robots.

## II. Design and Implementation

### *A. Design of the Soft and Reprogrammable Permanent Magnet*

The concept of the srPM is based on a permanent magnet setup having two operation states depending on its magnetic flux density. In the ON state, the srPM acts like a permanent magnet, and in the OFF state, the magnetic flux density of the srPM is reduced to zero. The srPM consists of one hard magnet, NdFeB, and one semi-hard magnet, AlNiCo, in the axisymmetric configuration as shown in Figure 1. It has NdFeB inside, and AlNiCo surrounding it with magnetorheological elastomer (MRE) caps at the poles. The AlNiCo and NdFeB magnets have similar remanence, so when the magnetization directions are opposite, their total magnetic flux density is nearly zero. The MRE caps are used to efficiently direct magnetic flux inside the srPM.

The volume ratio of the flexible magnets and the geometry of the srPM are two important design parameters. The volume ratios of the flexible magnets are chosen to maximize the flux density of the srPM in the ON state. The geometry of the srPM is determined by the finite element analysis given in Sec. III-D to minimize the flux density of the srPM in the OFF state. Based on these analyses, the NdFeB magnet core diameter is set at 2 mm and the AlNiCo outer diameter is set at 4 mm. The total length of the srPM is 6 mm with a diameter of 4 mm.

### *B. Fabrication of the srPM*

The srPM consists of three materials: flexible AlNiCo, flexible NdFeB magnets, and MRE caps. Flexible AlNiCo is made

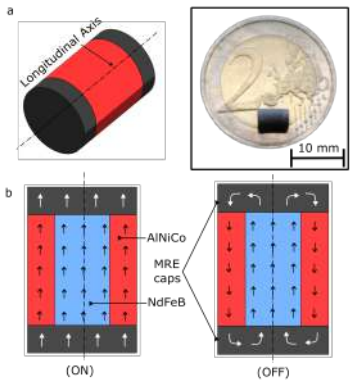


Fig. 1. Soft and reprogrammable permanent magnet. (a)The design of the srPM is axially symmetric. It consists of a cylindrical NdFeB composite, a hollow AlNiCo composite, and two MRE caps at the ends. A fabricated sample of the srPM, which has a length of 6 mm and a diameter of 4 mm, on a 2€. (b) In the ON state (left), the magnetization direction of the NdFeB and the AlNiCo are the same, resulting in a high magnetic field. In the OFF state (right), the magnetization directions are opposite and counteract each other, resulting in a near-zero field. The black arrows indicate remanent magnetization.

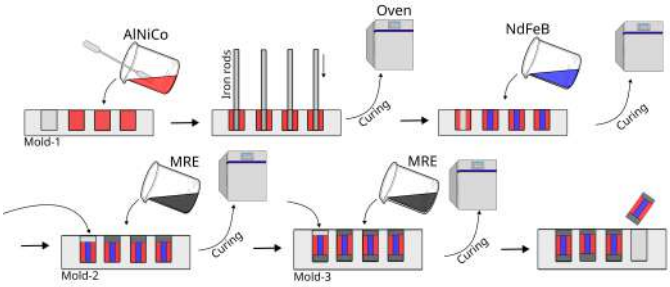


Fig. 2. Fabrication processes: Mixed and degassed uncured Alnico mixture is poured into the first mold, and metal rods are inserted for the NdFeB opening. After it is cured in the oven and the metal rods are removed, the cured and degassed NdFeB mixture is poured into the holes formed by the metal rods. Afterward, the NdFeB and AlNiCo mixtures are cured in the oven, the srPMs are removed from the first mold with a pair of tweezers gently, and they are placed in the second and third molds, subsequently for MRE caps, and the same procedure is performed for MRE caps.

of Dragon Skin 30 (Smooth-On Inc.) and AlNiCo powder (American Elements). Dragon Skin with AlNiCo powder of a 40% volume ratio is added together and mixed until homogeneous. The mix is poured into a 3D-printed acrylonitrile styrene acrylate mold. The mold is placed at 80 °C oven for 30 minutes to cure. After the flexible AlNiCo magnet is cured, it is replaced in another mold for a flexible NdFeB magnet. The same process is also used for the NdFeB magnet with NdFeB powders (QP-S-11-9-20001, Magnequench, Co. Ltd.). NdFeB mixture is poured on the mold, which AlNiCo magnet is replaced, and it is placed at 80 °C oven for 30 minutes to cure. Pouring the mixture on top of the cured part eliminates the need for adhesive. The same procedure is repeated for MRE caps with carbonyl iron particles (CIP) (Nanokar). MRE parts are poured at the end of the AlNiCo and NdFeB parts in two stages. In the first stage, only one side is cured, and in the second stage, the other MRE cap of the srPM is cured.

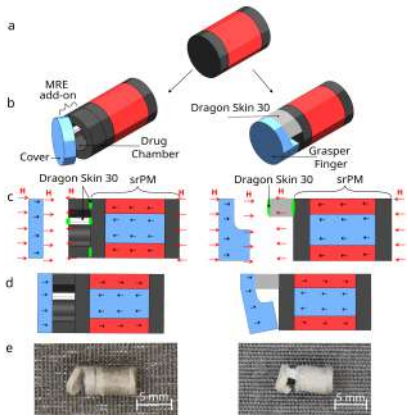


Fig. 3. Two robotic applications of the soft and reprogrammable permanent magnet. Blue regions indicate NdFeB, and red regions indicate AlNiCo composites. Black arrows indicate remanent magnetization in the material, and the red arrows indicate the externally applied magnetic field. (a) A single srPM. (b) Schematics of the capsule robot (left) and the grasper (right). (c) An MRE capsule chamber and an MRE add-on are attached to the robots with the Silpoxy. The NdFeB chamber cover and the srPM are separately magnetized with magnetic field H. The NdFeB grasper finger and the srPM are separately magnetized in opposite directions. The chamber cover and the grasper finger are assembled with Silpoxy. The assembled state refers to the ON state, where the capsule chamber cover and the grasper finger are in the open position. (d) After a magnetic pulse is applied to change the magnetization direction of the AlNiCo magnet, the srPM turns to an OFF state, resulting in the closure of the lid and the gripper (e). The prototypes of the capsule and the grasper. They are shown when they are in the open position.

### C. Magnetization of the srPM

The srPM is initially magnetized with a custom-made pulse magnetizer. The pulse magnetizer uses capacitor discharge energy to create a magnetic pulse inside a coil with a 20 mm inner diameter, where the coil compromises 100 wraps of insulated copper wire with a 1.5 mm diameter. Two capacitors ($450V$ $470\mu F$) are utilized to discharge the energy over the coils. After the initial magnetization, the magnetization directions of the AlNiCo magnet and the NdFeB magnet are the same. Thus, the SrPM is in the ON state.

To change the state of the srPM, a 180 mT magnetic field is required to change the magnetization direction of the AlNiCo magnet without completely affecting the NdFeB magnet. The magnetization direction of the AlNiCo magnet can be changed by an external short-duration, low-energy magnetic pulse. A custom-built electromagnet assembly consisting of two electromagnets is used to change the state of the srPM. The srPM is placed between the two electromagnets, and capacitor discharge energy is used to create a magnetic pulse across the coils. Each electromagnet coil consists of 1000 turns of copper wire with 0.8 mm diameter on a 45 mm diameter permalloy 80 core. The magnitude of the magnetic pulse required to change the magnetization of the semi-hard AlNiCo magnet is approximately 200 mT. The required capacitor discharge energy is 42.3 J, and the power is 4.23 kW. The pulse duration is 10 ms.

### D. Robotic Applications

We have implemented the srPM in two milli-scale soft robots for medical applications: (1) a soft magnetic capsule for

targeted drug delivery and (2) a soft grasper for non-invasive *in-vivo* manipulation. The srPM-based magnetic capsule is composed entirely of soft components that promise active functions for targeted drug delivery, biopsy and therapeutics. The srPM-based grasper uses magnetic forces to open and close a gripper. It can be used for biopsy or fixation.

*1) Soft Magnetic Capsule:* The capsule robot consists of an srPM and a flexible NdFeB magnet whose magnetizations are opposite. The magnetizations of the srPM and the flexible NdFeB magnet are opposite. Thus, when the srPM is in the ON state, the srPM and the magnet push against each other, and the capsule is opened. When the srPM is in the OFF state, the magnetic MRE cap attracts the NdFeB cover, and the capsule is closed. For the capsule robot, the srPM is extended with a 2 mm thick hollow MRE cylinder with a 6.2 $mm^3$ cavity in the center, which works as a drug chamber. The drug chamber is closed with a flexible NdFeB cover of 1 mm in height and 4 mm in diameter. To produce the NdFeB cover, NdFeB powders with a 40% percent volume ratio are mixed with Dragon Skin 30. The NdFeB cover and the srPM are magnetized in opposite directions and stuck together with a support leg serving as a hinge with Dragon Skin 30. The leg that holds the NdFeB magnet is made from Dragon Skin 30. The silicone legs are fixed inside the cavity of the MRE cap with the Silpoxy. The magnetized NdFeB cover was placed on the Dragon Skin leg and fixed with Silpoxy. The NdFeB cover is attached to the cavity with a Dragon Skin 30 rubber leg. Before the assembly is completed, the srPM and the NdFeB cover are magnetized separately in opposite directions. The magnetization of the srPM and the flexible NdFeB magnet are opposite. Thus, when the srPM is in the ON state, the srPM and the magnet push against each other, and the capsule is opened. When the srPM is in the OFF state, the magnetic MRE cap attracts the NdFeB cover, and the capsule is closed. The shape of the MRE cap and the thickness of the NdFeB cover are designed to hold at least two grams of a drug inside during locomotion. An illustration of the capsule robot and the working principle can be seen in Figure 3 (the left column).

*2) Soft Grasper:* The grasper consists of an srPM and a flexible NdFeB magnetic finger. When the srPM is in the ON state, the magnetization direction of the NdFeB finger is opposite to that of the srPM, resulting in a repulsive force between them. This repulsion causes the gripper finger to move away, opening the gripper. When a magnetic pulse is applied to switch the srPM to the OFF state, its total magnetization approaches zero, eliminating the repulsive force. At this point, an attractive force between the NdFeB finger and the MRE cap causes the NdFeB finger to deform, closing the gripper. A Dragon Skin 30 rubber spacer is attached to the top of the srPM module. The NdFeB finger is positioned on top of the rubber spacer. The Dragon Skin, which makes the NdFeB finger stand out, was cut from 1.25 mm thin layers cured in an aluminum mold. The Dragon Skin is stuck to srPM with Silpoxy. An NdFeB cover is manufactured with a 40% percent volume ratio with Dragon Skin by curing it in a cylindrical mold with a 1 mm height. A full cylinder NdFeB and a cut notch are merged into one, forming a grasper finger. At this stage, srPM and NdFeB fingers are separately magnetized in the reverse direction and stuck together with Silpoxy.

## III. Characterization and Simulation

The magnetic and mechanica properties of the flexible components comprising the srPM are evaluated before the design is finalized.

### A. Magnetic Characterization of the srPM

The magnetic measurements are taken for three srPM samples, each in ON and OFF states, on both sides, with five points per side. In the ON state, the magnetic field exerted by the module is 22.72 mT on average with a standard deviation of 0.35. In the OFF state, the magnetic field exerted by the module is 3.23 mT on average with a standard deviation of 0.26.

*1) Matrix Material Experiment:* The matrix materials of the magnetic soft materials have great importance based on their mechanical properties and chemical stability. Since the prior studies suggest that the particles may rotate inside the elastomeric matrix [42], an experiment is designed to see how hard magnetic materials act on different matrix materials. Four matrix materials are tested to choose the appropriate one for this study. The first matrix material is Ecoflex 00-30 with low-viscosity (3000 cps) silicone oil. Silicone oil decreases viscosity at the uncured stage, facilitating the uniform mixing of magnetic powder into the elastomer and resulting in a softer, more flexible magnet after curing. The other matrix materials are Ecoflex 0030, Dragon Skin 30, and Sil 960. Cylindrical, flexible magnets with 10 mm diameter and 16 mm length were manufactured with different matrix configurations for AlNiCo and NdFeB. All flexible magnets include a 40% volume ratio of magnet powders. Matrix compositions are EcoFlex 0030 with a 20% weight ratio of silicone oil, EcoFlex 0030, Dragon Skin 30, and Sil 960, respectively. Prior to the test, all the samples are magnetized. Flexible magnets are exposed to pulses of varying magnitudes in the direction opposite to their magnetization, and their remanent magnetization is then measured. Magnitudes of the pulses are 0, 5, 10, 15, 20, 25, 30, 40, 60, 80, 100, 120, and 150 mT, respectively. Three samples were tested from each matrix powder configuration, and six values were read from the flexible magnet's north and south surfaces from random points. The results given in Figure 4 indicate that as matrix materials get softer, the remanence magnetization of the flexible magnet decreases, and the flexible magnet becomes more susceptible to the applied magnetic field. The sample with silicone oil is affected most by the applied magnetic field. These results give clues about the reason for the sensitivity of the applied magnetic field. Adding silicone oil decreases the density of the cross-links in the polymer; this makes the polymer softer and easier to tear. Moreover, high viscosity of the Sil 960 prevents homogenous mixing of the elastomer with magnetic particles.

*2) SEM Analysis:* To solidify the results obtained from the matrix material experiment, samples were scanned under the scanning electron microscope (SEM). The SEM images were collected with back-scattered electrons mode. The SEM images of flexible NdFeB and AlNiCo magnets with matrix

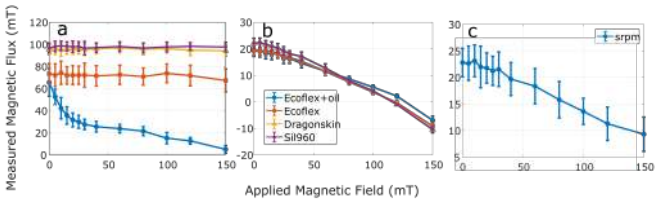


Fig. 4. Results of the matrix material experiments for (a) flexible NdFeB magnets and (b) flexible AlNiCo magnets, (c) and the srPM. Each point is the mean of three specimens, and the error bar represents the standard deviation.

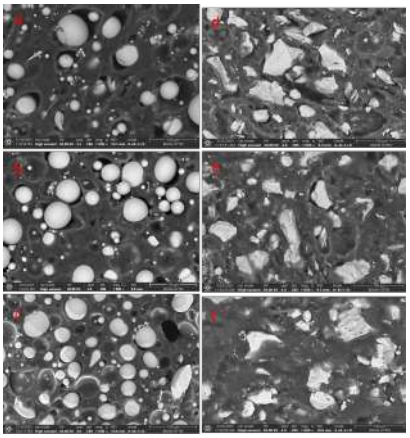

Fig. 5. SEM images of the NdFeB and AlNiCo samples are shown. The first column displays NdFeB samples, while the second column shows AlNiCo samples. The top row (a, d) represents samples with EcoFlex containing silicone oil, the middle row (b, e) shows EcoFlex without oil, and the bottom row (c, f) displays samples made with Dragon Skin. The images are 1000 times magnified.

materials of Ecoflex 0030 with oil, Ecoflex 0030 without oil, and Dragon Skin 30 without oil with a magnification of 1000 times can be seen in Figure 5. SEM images reveal that there are cavities around the powders in the samples that contain silicone oil. AlNiCo particles in the sample containing silicone oil catch the elastomer matrix, despite the cavities, thanks to their uneven shapes; however, the NdFeB particles seem free to rotate inside the matrix due to their spherical shape. This observation supports the results of the matrix material experiments, which showed minimal changes in the behavior of AlNiCo magnets, whereas the NdFeB magnets exhibited more significant differences. Those results indicate that the change in the remanence magnetization after exposure to low magnetic fields is probably caused by the physical movements of the particles rather than the particles' internal magnetic domains.

*3) VSM Experiment:* The magnetic properties of flexible magnets are the most important factor in the performance of srPM. The magnetic properties of the NdFeB particles (of spherical shape, 50 $\mu$m in diameter) and their composite are obtained from the manufacturer data [43]. However, detailed magnetic properties of the purchased AlNiCo powder are not available. Since the full magnetization curve is needed for the state change of the flexible AlNiCo magnet and for simulation purposes, the hysteresis curves of the flexible AlNiCo powders and flexible magnets were obtained using a Vibrating Sample Magnetometer (VSM) (Quantum Design PPMS 9T). Key findings from the analysis include the remanence and coercivity values of the flexible magnets: approximately 150 mT and 50 kA/m for flexible AlNiCo and 300 mT and 250 kA/m for flexible NdFeB, respectively. These magnetic properties are used for magnetic simulations of the srPM. From those experiments, Ecoflex 0030 and Dragon Skin are the best candidates for matrix materials, and Dragon Skin outperforms Ecoflex 0030 as the NdFeB matrix in the matrix material experiment. Thus, Dragon Skin is chosen as the matrix material.

### *B. Mechanical Characterization of the srPM*

Mechanical characterization is essential for the design of robots based on the srPM. These tests are performed using a custom-built tensile test platform designed for precision and control. The platform is built on linear rails and is controlled by a micrometer driven by a Nema 17 stepper motor controlled by an Arduino Uno. Motion is transmitted via a belt and pulley system that connects the stepper motor to the micrometer. A 500 g capacity load cell (DigiKey) is used for force sensing, and 3D-printed fixtures are used to securely mount the specimens. A 2D digital image correlation (DIC) technique is used to analyze the deformation. The specimens are speckled with spray dye to create a pattern to track local deformations. A high-resolution CCD camera (Pike F505B, Allied Vision Technologies) captures images for this analysis. The results of the tensile test, , indicate that the material exhibits a slightly nonlinear behavior with a small hysteresis during the loading and unloading cycles.

DIC samples of MRE were manufactured using silicone rubber and carbonyl iron particles. Two parts of the silicone rubber are mixed to fabricate matrix materials. After matrix materials were mixed, a volume ratio of 40% CIP was added to the mixture and blended till gets homogenous (around 2 minutes). The mixture was placed in a vacuum chamber for 3 minutes to degassing. The mixture was poured into 3D-printed molds and cured in the 80 °C oven for 30 minutes. The same procedures were repeated for AlNiCo and NdFeB particles.

### *C. Force Applied by the srPM*

To evaluate the performance of the srPM, the force it applies to an iron piece is measured in both its ON and OFF states. The test is conducted with the same test setup with the mechanical characterization test with some modifications. The srPM is attached to a 100 g load cell (DigiKey) on one end while the other end remains free to move and touch the iron piece. The load cell and the srPM assembly are allowed to move toward a fixed iron piece, and force measurements are recorded at the point of contact. In the ON state, the srPM exerts a force of 19 mN, with a standard deviation of 0.38 mN. In the OFF state, the force decreases to 7 mN, with a standard deviation of 1.1 mN.

### D. Simulation of the srPM

Magnetic simulations are conducted using ANSYS Maxwell. The flexible AlNiCo and NdFeB components are modeled as simple permanent magnets, with their properties characterized using values obtained from VSM analyses. The MRE parts are modeled as soft magnets.

To validate the srPM model in the simulations, an iron piece is placed at the bottom of the srPM with a 0.1 mm air gap to measure how it is affected by the magnetic field generated by the srPM. The diameters of the flexible magnets are selected as design parameters, while the magnetic forces are used as the cost function. The magnetic force in the OFF state should be low enough that the magnet cannot support its own weight, whereas it is aimed to be maximized in the ON state. The geometry of the srPM is finalized in line with the result. The calculated attraction forces between the iron piece and the srPM module are 18 mN in the ON state and 5 mN in the OFF state, aligning closely with the experimental results in Section III-C. For the capsule robot in the ON state, the srPM generates a repelling force of 53 mN and an attracting force of 46 mN on the cover. For the gripper robot, the repelling and attracting forces are calculated as 15 mN and 26 mN, respectively.

To assess whether these forces are sufficient to bend the gripper finger for grasping, mechanical simulations are performed. The material properties for these simulations are derived from DIC-assisted tensile testing experiments.

## IV. Evaluation and Demonstration

### A. Robot Capabilities

This study presents two robotic applications, namely the soft magnetic capsule and the soft grasper, in order to demonstrate the capabilities of the srPM. A series of experiments were conducted on the capsule and the grasper to demonstrate their potential for future medical applications.

The primary functions of the targeted drug delivery capsule are twofold: firstly, to seal a package, and secondly, to deliver it to its destination. To facilitate the testing of the capsule, it is first filled with blue food colouring (dye), closed to seal it, and then placed within a glass container filled with water. The capsule is then moved within the container in the presence of an external magnetic field of approximately 5 mT, thereby demonstrating its locomotion capability and the absence of leakage. Following the leakage test, the container is placed between the electromagnets described in Section II-C to demonstrate how it is opened up to release its package. The capsule is then exposed to a 200 mT magnetic field, which is used to trigger the desired response. The experimental footage can be viewed in Figure 6.

The grasper uses magnetic forces to open and close a gripper for potential biopsy or fixation applications. Therefore, the gripping force of the gripper is measured. Measurements were performed on different specimens to account for the effect of friction between the gripper and the specimen, as well as the geometry of the specimens. Different types of paper with different thicknesses are used for thin samples. The papers are textured paper (0.25 mm), sandpaper (0.15 mm), and cardboard (1.25 mm). The results are 1.8 g, 1.3 g, and 6.8 g, respectively. Different sizes of copper wire are used for wire-like materials. The results are 1.6 g for 2 mm diameter wire and 2.6 g for 1 mm diameter wire.

### B. Demonstration

A wrinkled, tissue-like silicone phantom is manufactured using silicone rubber (RTV-2 Mold Silicone, Aydın Kompozit). It is used to demonstrate the capabilities of both robots: the soft magnetic capsule and the soft grasper.

The capsule robot is navigated to the target area on the phantom using manually-controlled permanent magnets placed beneath the phantom. The movement of the robots is achieved by rotating a permanent magnet of size 10 x 40 x 40 mm to create a rotating magnetic field. The magnitude of the field is around 10 mT. Then, the electromagnets described in II-C are placed manually in a way that the magnetic field to be applied is aligned with the longitudinal axis of the srPM. Once positioned, the capsule is fixed to the phantom by applying a magnetic field perpendicular to the capsule magnetization axis for a clear view of its drug chamber cover. A pulsed magnetic field amplitude of 200 mT is then applied to the capsule using the electromagnets to actuate the srPM, triggering the release mechanism and opening the cover to simulate drug delivery.

The scenario for the grasper is to grip a splinter (a copper wire) embedded in the phantom. The grasper is guided to the splinter using the external permanent magnets located under the phantom. Both position and orientation are important for the grasper as it needs to grip the target with its finger. During this movement, a 5 mT magnetic field is applied to the grasper. Once the target is reached, the grasper grips the splinter securely by actuating the srPM. To stabilize the position of the grasper, a magnetic field perpendicular to its magnetization direction is applied to lock it in place. A perpendicular magnetic field is required for a robot to preserve its position; otherwise, it will sway with the applied magnetic pulse. Finally, the electromagnets apply a pulsed magnetic field amplitude of 200 mT to grip the splinter firmly.

## V. Discussion and Conclusion

In this study, a novel concept for *in-vivo* magnetic reprogramming and reconfiguration of small-scale soft robots is proposed that goes beyond the current state of the art

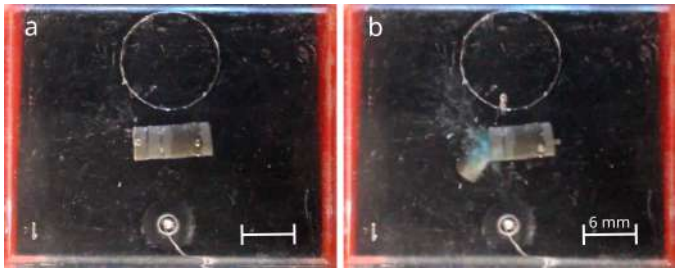


Fig. 6. Demonstration of the soft magnetic capsule underwater. (a) The capsule is closed to seal the package inside, and (b) it is opened to release the package. The blue colour is a dye representing the package.

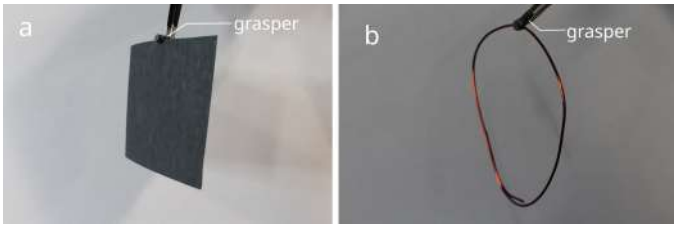


Fig. 7. Gripping force measurement setup. The grasper is tested while carrying various specimens: (a) a sandpaper of 1.3 g, and (b) a copper wire of 2.6 g.

by eliminating the heat requirement and by enabling reprogramming under only a magnetic field. We introduce a soft counterpart to the classical electro-permanent magnet. Unlike the classical EPM, this reprogrammable permanent magnet is soft and designed to operate without a coil for remote control functionality. It is suitable for on-board use in magnetic soft robots either to modify the magnetic properties of such robots or to actuate certain functionalities. By enabling remote state change, the srPM allows soft magnetic robots to perform specific tasks without physical tethering, complementing their untethered steering capability. This is our main and most significant contribution to the current state of the art in this study.

In addition, the srPM is cost-effective and can be easily fabricated for various applications. Operating with minimal energy consumption makes the srPM a practical solution for various applications including medical robotics.The energy consumption is related to the srPM design, i.e., the required magnetic field to magnetize the AlNiCo, which is specific to the material type. A low coercivity AlNiCo grade requires a low magnetic field, resulting in low energy demand. The proposed reprogramming strategy has significantly lower energy consumption than the heating-based reprogramming strategies, which consume around 1400 J just for heating the material [32].

Towards this goal, we developed two untethered millimeter-scale robots based on the proposed novel srPM: a capsule robot and a medical grasper. The developed srPM measures 6 mm in length and 4 mm in diameter. The robots match this diameter and are 10 mm in lenght. These robots can be remotely controlled and can switch states with a short duration, low energy external magnetic pulse.

In the two robotic applications, switching between ON and OFF states could have also been achieved by using soft magnetic composites instead of the proposed srPM. The advantage of using srPM is that the magnetic field around the srPM is close to zero when it is in the OFF state. Thus, it does not cause any repulsion or attraction forces at the OFF state. Some applications, such as a valve for ferrofluids, magnetic jamming, or maybe self-assembling robots, can benefit from this property. Although the selected application scenarios in this study do not necessarily benefit from this property, they are feasible enough to show the capabilities of the srPM. Further and more complex applications are left as future work.

The state of the srPM can be switched with a single magnetic pulse, which provides low energy consumption. However, despite the low energy requirement, the magnetic pulse is of high magnitude, requiring significant power. Powering the electromagnets directly from a power supply would require a high-capacity power source, which is typically bulky and expensive. Alternatively, we used a more efficient and cost-effective solution that is based on a capacitor and pulse generator to provide the required power. Alignment of the magnetic pulse with the srPM is critical for effective operation, which can be challenging. This alignment problem can be overcome by increasing the amplitude of the pulse or applying magnetic fields in different orientations. For more precise control, the magnetic signature of the robot can be tracked by magnetic sensors over the body.

Another important result of this study is the demonstration of the mechanical movement of particles embedded in the elastomer matrix. The rotation of these particles depends on both the properties of the elastomer matrix and the shape of the particles. If these factors can be tuned so that rotation occurs only after a certain threshold, this could be used for magnetic programming of soft magnetic robots.

The proposed magnetic robots and srPM hold great promise for future medical applications such as targeted drug delivery and minimally invasive surgery. Their simple design allows for easy scaling and modification to meet specific needs. They are fabricated using straightforward manufacturing processes, making them cost-effective and accessible for a wide range of untethered procedures. The absence of potentially hazardous components, such as batteries, enhances their safety in the event of an accident. One of their most notable features is their low energy consumption, which further contributes to their practicality and efficiency in medical settings. Although the remote and untethered reprogrammability and control of the robots is a promise for in-vivo applications, biocompatibility of the materials must be addressed as future work. The biocompatibility of the magnetic powders used in this study can be a problem, especially for relatively long exposures. To surmount this, powders can be coated with biocompatible materials like silica. Instead of Silpoxy, uncured Dragon Skin can be used as an adhesive for biocompatibility. Besides the promise for in-vivo application, their low energy consumption further contributes to their practicality and efficiency in a possible medical setting.

## REFERENCES

[1] H.-W. Huang, M. S. Sakar, A. J. Petruska, S. Pané, and B. J. Nelson, "Soft micromachines with programmable motility and morphology," *Nature Communications*, vol. 7, p. 12263, 7 2016.

[2] Z. Ren, W. Hu, X. Dong, and M. Sitti, "Multi-functional soft-bodied jellyfish-like swimming," *Nature Communications*, vol. 10, p. 2703, 7 2019.

[3] H. Gu, Q. Boehler, H. Cui, E. Secchi, G. Savorana, C. D. Marco, S. Gervasoni, Q. Peyron, T.-Y. Huang, S. Pane, A. M. Hirt, D. Ahmed, and B. J. Nelson, "Magnetic cilia carpets with programmable metachronal waves," *Nature Communications*, vol. 11, p. 2637, 5 2020.

[4] W. Hu, G. Z. Lum, M. Mastrangeli, and M. Sitti, "Small-scale soft-bodied robot with multimodal locomotion," *Nature*, vol. 554, pp. 81–85, 2 2018.

[5] T. Xu, J. Zhang, M. Salehizadeh, O. Onaizah, and E. Diller, "Millimeter-scale flexible robots with programmable three-dimensional magnetization and motions," *Science Robotics*, vol. 4, 4 2019.

[6] Y. Kim, H. Yuk, R. Zhao, S. A. Chester, and X. Zhao, "Printing ferromagnetic domains for untethered fast-transforming soft materials," *Nature*, vol. 558, pp. 274–279, 6 2018.

[7] H. Gu, Q. Boehler, D. Ahmed, and B. J. Nelson, "Magnetic quadrupole assemblies with arbitrary shapes and magnetizations," *Science Robotics*, vol. 4, 10 2019.

[8] X. Zhao and Y. Kim, "Soft microbots programmed by nanomagnets," *Nature*, vol. 575, pp. 58–59, 11 2019.

[9] H. Lee, Y. Jang, J. K. Choe, S. Lee, H. Song, J. P. Lee, N. Lone, and J. Kim, "3d-printed programmable tensegrity for soft robotics," *Science Robotics*, vol. 5, 8 2020.

[10] Z. Qi, M. Zhou, Y. Li, Z. Xia, W. Huo, and X. Huang, "Reconfigurable flexible electronics driven by origami magnetic membranes," *Advanced Materials Technologies*, vol. 6, 4 2021.

[11] T. Kawasetsu, T. Horii, H. Ishihara, and M. Asada, "Mexican-hat-like response in a flexible tactile sensor using a magnetorheological elastomer," *Sensors*, vol. 18, p. 587, 2 2018.

[12] Y. Zhao, S. Gao, X. Zhang, W. Huo, H. Xu, C. Chen, J. Li, K. Xu, and X. Huang, "Fully flexible electromagnetic vibration sensors with annular field confinement origami magnetic membranes," *Advanced Functional Materials*, vol. 30, p. 2001553, 6 2020.

[13] S. Yim, E. Gultepe, D. H. Gracias, and M. Sitti, "Biopsy using a magnetic capsule endoscope carrying, releasing, and retrieving untethered microgrippers," *IEEE Transactions on Biomedical Engineering*, vol. 61, no. 2, pp. 513–521, 2014.

[14] Y. Kim, G. A. Parada, S. Liu, and X. Zhao, "Ferromagnetic soft continuum robots," *Science Robotics*, vol. 4, no. 33, p. eaax7329, 2019. [Online]. Available: https://www.science.org/doi/abs/10.1126/scirobotics.aax7329

[15] G. Ciuti, P. Valdastri, A. Menciassi, and P. Dario, "Robotic magnetic steering and locomotion of capsule endoscope for diagnostic and surgical endoluminal procedures," *Robotica*, vol. 28, no. 2, p. 199–207, 2010.

[16] S. E. Chung, X. Dong, and M. Sitti, "Three-dimensional heterogeneous assembly of coded microgels using an untethered mobile microgripper," *Lab Chip*, vol. 15, pp. 1667–1676, 2015. [Online]. Available: http://dx.doi.org/10.1039/C5LC00009B

[17] H. Ceylan, J. Giltinan, K. Kozielski, and M. Sitti, "Mobile microrobots for bioengineering applications," *Lab Chip*, vol. 17, pp. 1705–1724, 2017. [Online]. Available: http://dx.doi.org/10.1039/C7LC00064B

[18] B. J. Nelson, I. K. Kaliakatsos, and J. J. Abbott, "Microrobots for minimally invasive medicine," *Annual Review of Biomedical Engineering*, vol. 12, no. 1, pp. 55–85, 2010. [Online]. Available: https://doi.org/10.1146/annurev-bioeng-010510-103409

[19] M. Sitti, H. Ceylan, W. Hu, J. Giltinan, M. Turan, S. Yim, and E. D. Diller, "Biomedical applications of untethered mobile milli/microrobots," *Proceedings of the IEEE*, vol. 103, pp. 205–224, 2015.

[20] M. Sitti, "Miniature devices: Voyage of the microrobots," *Nature*, vol. 458, pp. 1121–1122, 2009.

[21] H. Lu, M. Zhang, Y. Yang, Q. Huang, T. Fukuda, Z. Wang, and Y. Shen, "A bioinspired multilegged soft millirobot that functions in both dry and wet conditions," *Nature Communications*, vol. 9, no. 1, pp. 3944–, 2018.

[22] A. N. Knaian, "Electropermanent magnetic connectors and actuators: devices and their application in programmable matter," Ph.D. dissertation, Massachusetts Institute of Technology, 2010.

[23] Z. Yang and L. Zhang, "Magnetic actuation systems for miniature robots: A review," *Advanced Intelligent Systems*, vol. 2, no. 9, p. 2000082, 2020. [Online]. Available: https://onlinelibrary.wiley.com/doi/abs/10.1002/aisy.202000082

[24] T. Leps, P. E. Glick, D. R. III, A. Parness, M. T. Tolley, and C. Hartzell, "A low-power, jamming, magnetorheological valve using electropermanent magnets suitable for distributed control in soft robots," *Smart Materials and Structures*, vol. 29, no. 10, p. 105025, sep 2020. [Online]. Available: https://dx.doi.org/10.1088/1361-665X/abadd4

[25] A. Gholizadeh, S. Abbaslou, P. Xie, A. Knaian, and M. Javanmard, "Electronically actuated microfluidic valves with zero static-power consumption using electropermanent magnets," *Sensors and Actuators A: Physical*, vol. 296, pp. 316–323, 2019. [Online]. Available: https://www.sciencedirect.com/science/article/pii/S0924424719301943

[26] A. D. Marchese, C. D. Onal, and D. Rus, *Towards a Self-contained Soft Robotic Fish: On-Board Pressure Generation and Embedded Electropermanent Magnet Valves*. Heidelberg: Springer International Publishing, 2013, pp. 41–54.

[27] J. I. Padovani, S. S. Jeffrey, and R. T. Howe, "Electropermanent magnet actuation for droplet ferromicrofluidics," *Technology*, vol. 04, no. 02, pp. 110–119, 2016. [Online]. Available: https://doi.org/10.1142/S2339547816500023

[28] K. J. McDonald, L. Kinnicutt, A. M. Moran, and T. Ranzani, "Modulation of magnetorheological fluid flow in soft robots using electropermanent magnets," *IEEE Robotics and Automation Letters*, vol. 7, no. 2, pp. 3914–3921, 2022.

[29] W. R. Johnson, S. J. Woodman, and R. Kramer-Bottiglio, "An electromagnetic soft robot that carries its own magnet," in *2022 IEEE 5th International Conference on Soft Robotics (RoboSoft)*, 2022, pp. 761–766.

[30] P. Zhang, M. Kamezaki, Z. He, H. Sakamoto, and S. Sugano, "Epm–mre: Electro permanent magnet–magnetorheological elastomer for soft actuation system and its application to robotic grasping," *IEEE Robotics and Automation Letters*, vol. 6, no. 4, pp. 8181–8188, 2021.

[31] L. T. Gaeta, K. J. McDonald, L. Kinnicutt, M. Le, S. Wilkinson-Flicker, Y. Jiang, T. Atakuru, E. Samur, and T. Ranzani, "Magnetically induced stiffening for soft robotics," *Soft Matter*, vol. 19, pp. 2623–2636, 2023. [Online]. Available: http://dx.doi.org/10.1039/D2SM01390H

[32] Y. Alapan, A. C. Karacakol, S. N. Guzelhan, I. Isik, and M. Sitti, "Reprogrammable shape morphing of magnetic soft machines," *Science Advances*, vol. 6, no. 38, p. eabc6414, 2020. [Online]. Available: https://www.science.org/doi/abs/10.1126/sciadv.abc6414

[33] G. Dong, Q. He, and S. Cai, "Magnetic vitrimer-based soft robotics," *Soft Matter*, vol. 18, pp. 7604–7611, 2022. [Online]. Available: http://dx.doi.org/10.1039/D2SM00893A

[34] H. Song, H. Lee, J. Lee, J. K. Choe, S. Lee, J. Y. Yi, S. Park, J.-W. Yoo, M. S. Kwon, and J. Kim, "Reprogrammable ferromagnetic domains for reconfigurable soft magnetic actuators," *Nano Letters*, vol. 20, no. 7, pp. 5185–5192, 2020, pMID: 32491865. [Online]. Available: https://doi.org/10.1021/acs.nanolett.0c01418

[35] H. Deng, K. Sattari, Y. Xie, P. Liao, Z. Yan, and J. Lin, "Laser reprogramming magnetic anisotropy in soft composites for reconfigurable 3d shaping," *Nature Communications*, vol. 11, no. 1, p. 6325, Dec 2020. [Online]. Available: https://doi.org/10.1038/s41467-020-20229-6

[36] W. Li, H. Chen, Z. Yi, F. Fang, X. Guo, Z. Wu, Q. Gao, L. Shao, J. Xu, G. Meng, and W. Zhang, "Self-vectoring electromagnetic soft robots with high operational dimensionality," *Nature Communications*, vol. 14, no. 1, p. 182, Jan 2023. [Online]. Available: https://doi.org/10.1038/s41467-023-35848-y

[37] Y. Sun, B. Sun, X. Cui, W. Li, Y. Zhang, L. He, S. Nong, Z. Zhu, J. Wu, D. Li, X. Li, S. Zhang, X. Li, and M. Li, "Addressable and perceptible dynamic reprogram of ferromagnetic soft machines," *Nature Communications*, vol. 16, no. 1, p. 2267, Mar 2025. [Online]. Available: https://doi.org/10.1038/s41467-025-57454-w

[38] O. Sodomka and F. Mach, "Electrically switchable magnetic elastomer," *AIP Advances*, vol. 15, no. 3, p. 035117, 03 2025. [Online]. Available: https://doi.org/10.1063/9.0000896

[39] W. R. Johnson and R. Kramer-Bottiglio, "Compliant electropermanent magnets," in *2024 IEEE 7th International Conference on Soft Robotics (RoboSoft)*, 2024, pp. 347–352.

[40] M. V. Vaganov, D. Y. Borin, S. Odenbach, and Y. L. Raikher, "Mesomagnetomechanics of hybrid elastomer composites: Magnetization of elastically trapped particles," *Journal of Magnetism and Magnetic Materials*, vol. 499, p. 166249, 2020. [Online]. Available: https://www.sciencedirect.com/science/article/pii/S0304885319326964

[41] G. V. Stepanov, D. Y. Borin, A. V. Bakhtiiarov, and P. A. Storozhenko, "Magnetic properties of hybrid elastomers with magnetically hard fillers: rotation of particles," *Smart Materials and Structures*, vol. 26, p. 035060, 3 2017.

[42] M. Vaganov, D. Borin, S. Odenbach, and Y. Raikher, "Effect of local elasticity of the matrix on magnetization loops of hybrid magnetic elastomers," *Journal of Magnetism and Magnetic Materials*, vol. 459, pp. 92–97, 2018. [Online]. Available: https://www.sciencedirect.com/science/article/pii/S0304885317321339

[43] Magnequench, "MQP-S-11-9-20001," accessed Jun. 3, 2017. [Online]. Available: https://mqitechnology.com/product/mqp-s-11-9-20001/